CANADA

DEPARTMENT OF MINES AND TECHNICAL SURVEYS

OTTAWA

MINES BRANCH INVESTIGATION REPORT IR 66-49

EXAMINATION OF TWO C.S.F. ICEBREAKER PROPELLER CASTINGS

by

D.E. PARSONS AND D.A. MUNRO

PHYSICAL METALLURGY DIVISION

COPY NO. 20

JUNE 21, 1966

Mines Branch Investigation Report IR 66-49

EXAMINATION OF TWO C.S.F. ICEBREAKER PROPELLER CASTINGS

by

D. E. Parsons* and D. A. Munro**

- - - - - -

SUMMARY OF RESULTS

Examination of two samples of fractured nickel-vanadium cast steel icebreaker propeller blades, manufactured by Canadian Steel Foundries Division, Montreal, P.Q., showed that both castings conformed exactly to the requirements of the specification (1963) and apparently conformed to standards of good workmanship with respect to soundness of section and quality of welds.

The tensile and Charpy V-notch properties met the specification and gave good mechanical results at ambient temperature.

However, drop-weight bars broken at low temperature, gave an NDT temperature of only -15°F despite Charpy V-notch energy values of the order of 80 ft-lb. Charpy V-notch bars did show evidence of cleavage despite high energy values.

It was recommended that the specification be reviewed to obtain minimum NDT temperature by elimination of vanadium and by control of the silicon and carbon contents to the requirements of the revised (June 1966) specification.

---

* Senior Scientific Officer and **Technician, Ferrous Metals Section, Physical Metallurgy Division, Mines Branch, Department of Mines and Technical Surveys, Ottawa, Canada.

INTRODUCTION

In December 1965, part of a broken cast steel propeller blade, removed from C.C.G.S. "Sir John A. MacDonald", was received from Department of Transport, Dartmouth, N.S., for metallurgical examination to determine the cause of failure. Subsequently, in January 1966, a small piece (blade-tip) broken from a second propeller was received by the Physical Metallurgy Division, Mines Branch, Department of Mines and Technical Surveys.

The two samples are identified as the "blade-stub" and "blade-tip" respectively, in this report.

ORIGIN AND IDENTIFICATION OF MATERIAL

Both propellers were cast nickel-vanadium steel manufactured at Canadian Steel Foundries Division, Hawker Siddeley Canada Ltd., Montreal, P.Q., Order No. 11975-65. The blade-stub sample is illustrated in Figure 1, as-received, and in Figure 2 after the fracture had been cleaned and derusted. The fracture surface was slightly pitted as a consequence of the broken propeller remaining in service for a period of three weeks after fracture. There is a clearly defined origin (arrow) indicated by the chevron markings. The fracture is fine-grained and uniform but without evidence of shear or deformation during failure so that failure appears to be due to brittle fracture caused by impact at sea water temperature.

Figures 4, 5 and 6 illustrate the appearance of the fracture and surface of the cast "blade-stub".

Figure 4(a) illustrates the "as-received", appearance of the fracture origin. Figures 4(b) and 4(c) illustrate the origin after cleaning of the fracture with $SbCl_3$ derusting solution. A chevron pattern pointing to the origin is illustrated. The presence of chevron markings is suggestive of brittle fracture under application of impact load. The surface has been slightly altered by pitting since fracture, due to operation of the blade-stub in sea water after failure of one blade and by subsequent outdoor storage.

Figure 5 illustrates a side-view and oblique surface view of the side surface of the propeller stub casting with the origin of the fracture marked by the arrows.

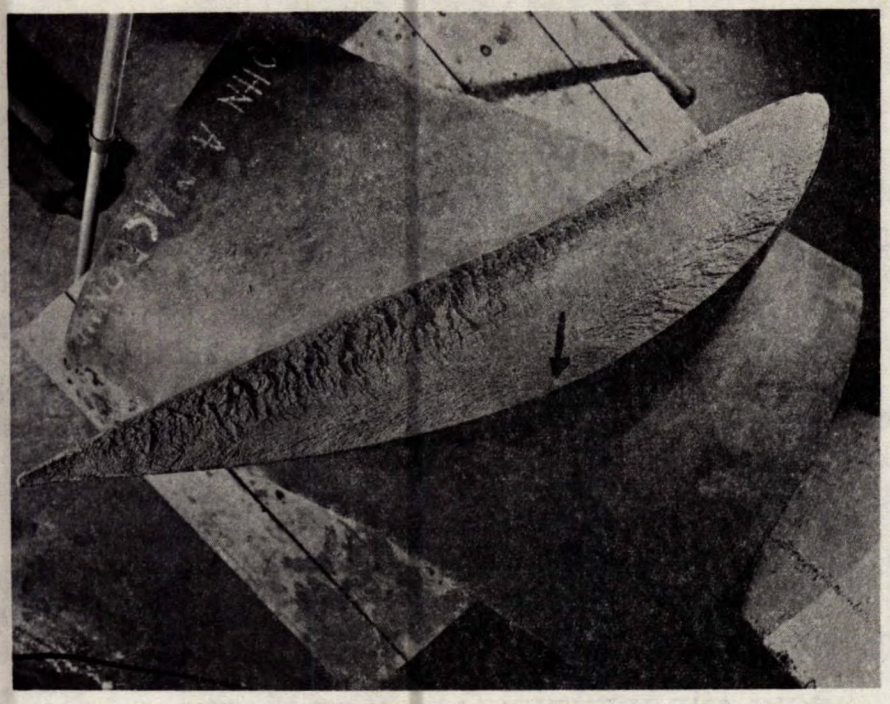

X 1/5 approx.

Figure 1. Broken "Blade-Stub", C.C.G.S. Sir John A. MacDonald. As-received. The origin of the fracture is shown by the arrow.

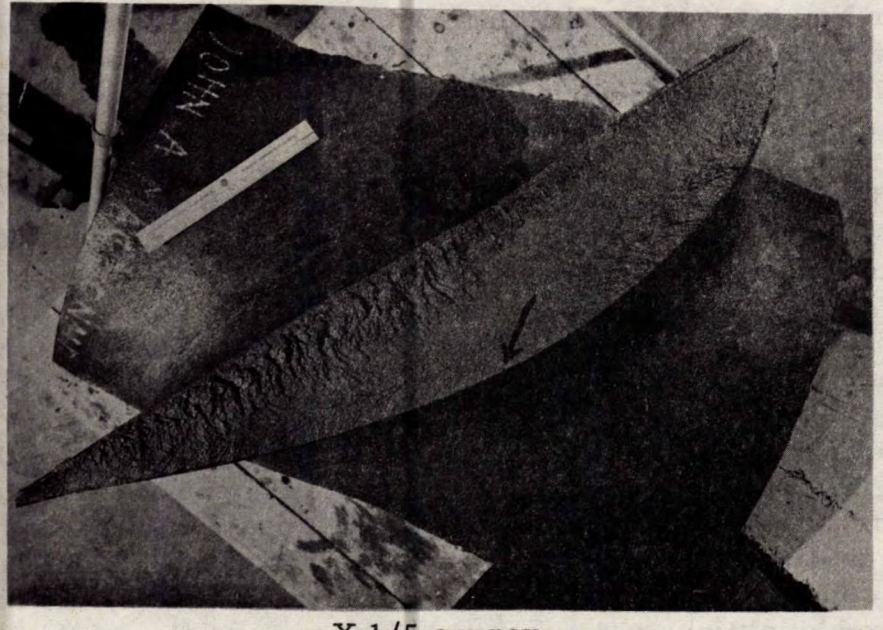

X 1/5 approx.

Figure 2. Broken "Blade-Stub", C.C.G.S. Sir John A. MacDonald. Cleaned and Derusted. The fracture surface is uniform and fine-grained but does not show evidence of deformation. The chevron pattern and origin suggest that failure occurred by brittle fracture under impact at sea water temperature.

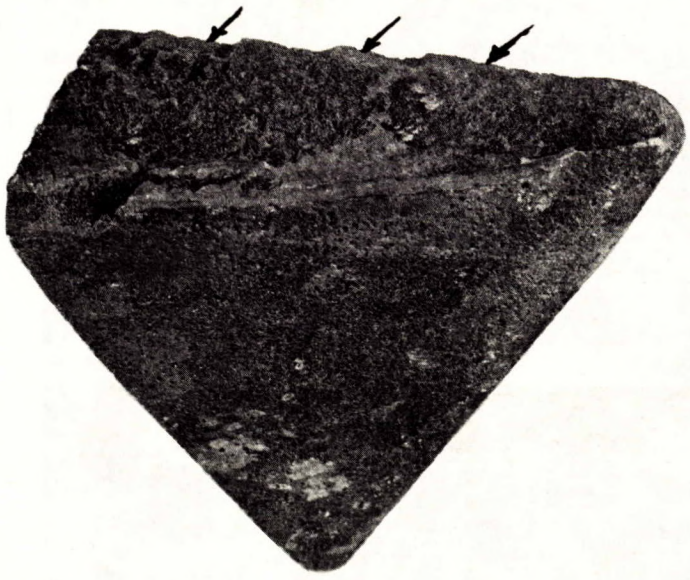

X 2/3 approx.

Figure 3. "Blade-Tip" Sample Submitted in January 1966, C.C.G.S. Sir John A. MacDonald. This picture illustrates part of a second broken blade from this ship. This blade exhibited more deformation during fracture as indicated by formation of a 1/8 in. shear-lip along the surface (arrows).

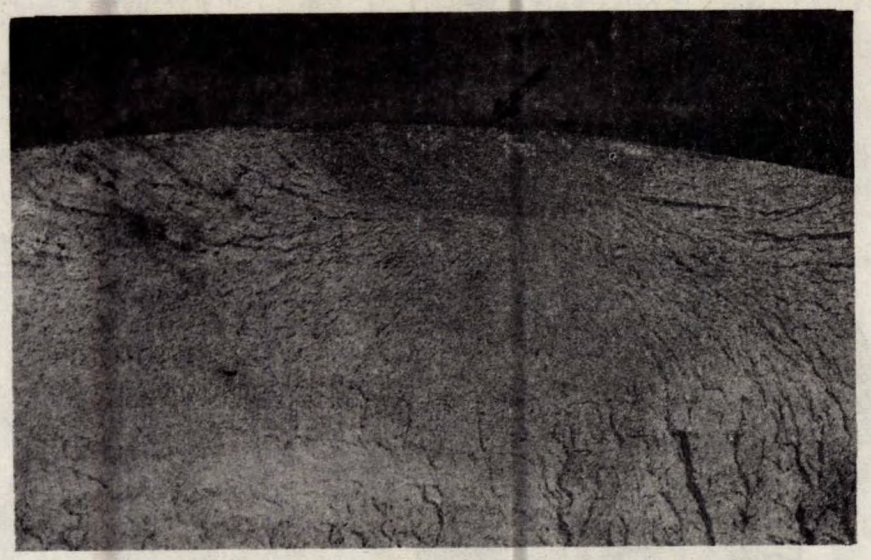

(a) X 1/3

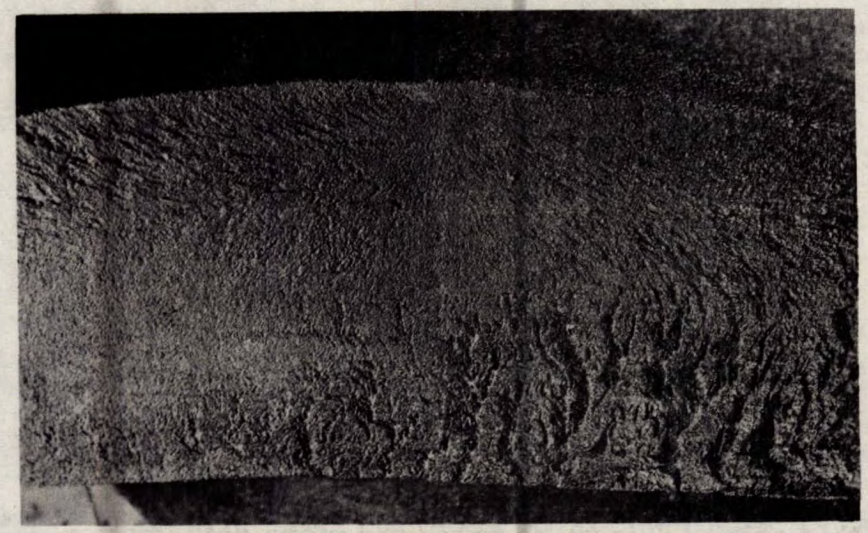

(b) X 1/4

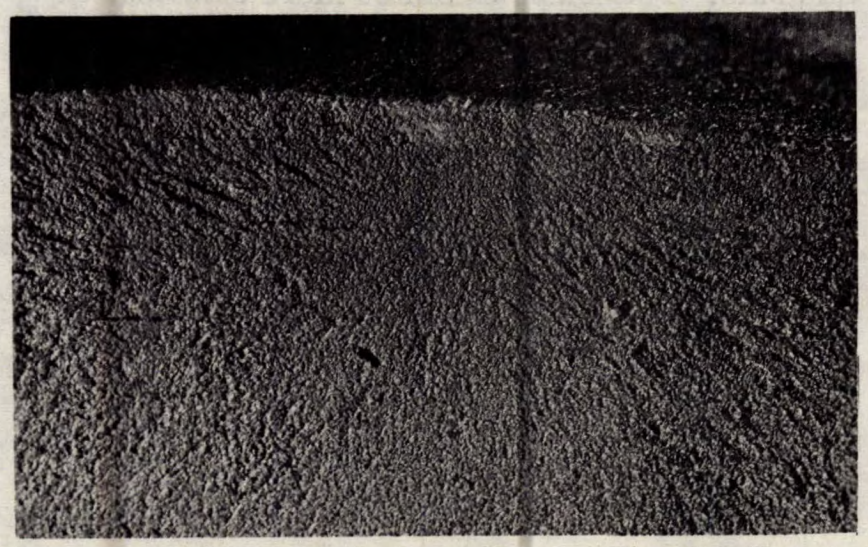

(c) X 1/3

Figure 4. Fracture Surface, Blade, Showing Fracture Origin
(a) as-received; (b) (c) derusted.

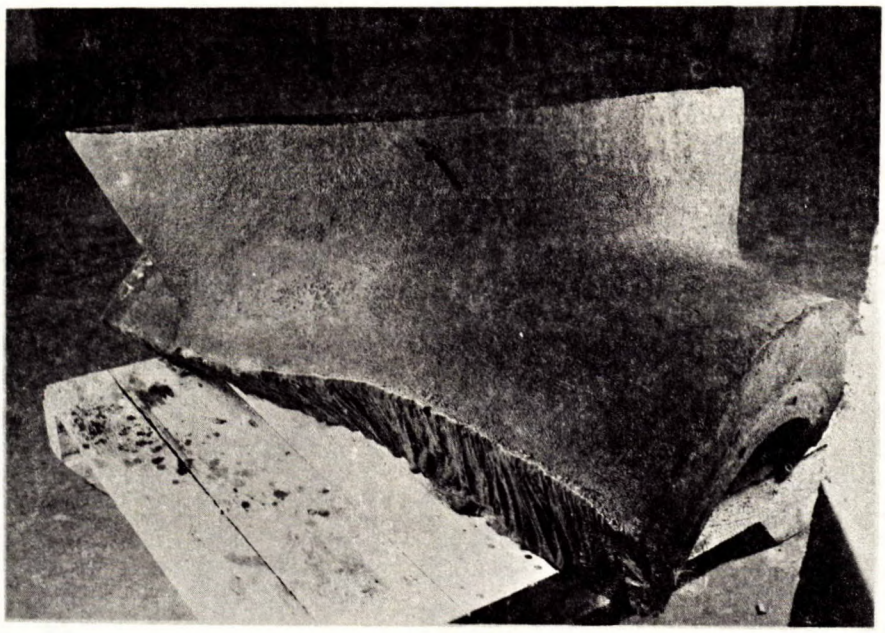

(a) Convex Surface-Elevation-Origin marked (arrow).

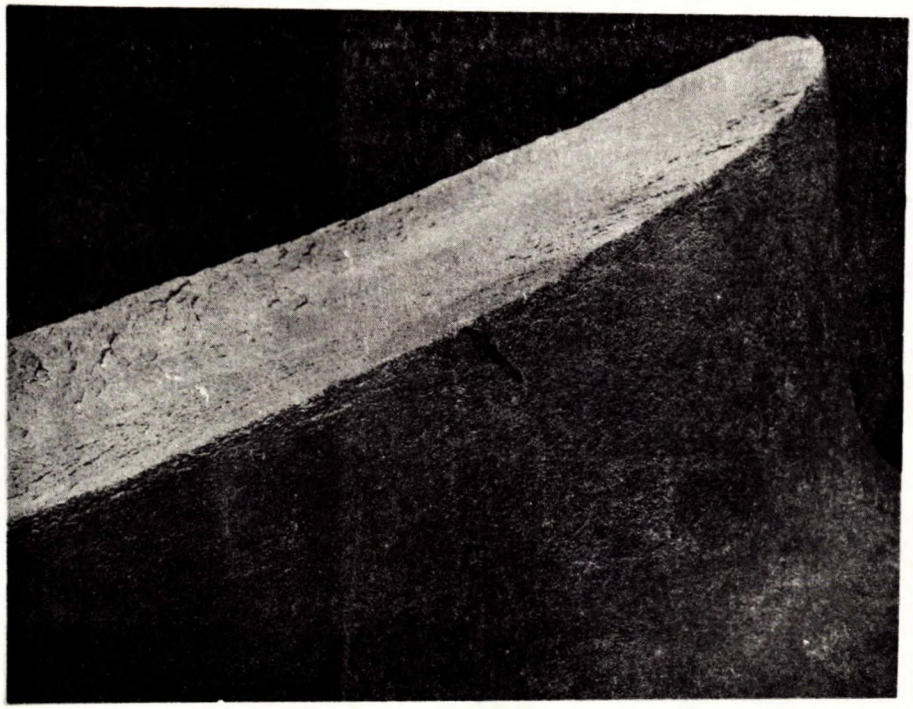

(b) Same side as (a) at higher magnification and showing fracture surface.

Figure 5. Convex Surface of Casting with Origin marked (arrow). Figure 5(a) shows the stub surface in elevation; Figure 5(b) shows the same surface at the origin with the origin visible on the fracture surface.

Figure 6(a) illustrates the concave surface of the blade-stub casting opposite to the failure surface. Figure 6(b) illustrates welds in the hub region which are visible as a result of etching by sea water. Unlike the welds illustrated, welds in the critical root area were not delineated by etching or metallography but were only visible on sulphur prints since the sulphur content of deposited weld metal was lower than that of the casting.

X 1/10 approx.

(a) Concave Side, Opposite to Origin.

(b) Welds in Non-Critical Hub Region - Etched by Service in Sea Water.

Figure 6. Concave Surface of Broken Blade-Stub. Figure 6(a) Welds are visible in the hub region; Figure 6(b) as etched by service in sea water.

METALLURGICAL EXAMINATION

Metallurgical examination was made as follows:

(i) Chemical Analysis - blade-stub and blade-tip samples.

(ii) Sectioning - Deep Etch and Sulphur Prints - Examination of Welds Relative to the Fracture Surface.

(iii) Mechanical Tests.

(iv) Drop-weight (NDT) and Charpy V-notch Impact Transition Test.

(v) Metallographic Examination.

Chemical Analysis

The results of chemical analysis are shown in Table 1.

Both broken propellers adhere closely to the chemical composition requirements of the 1963 specification for cast, nickel-vanadium steel propellers.

Sectioning

Sections were taken through the origin and for a distance of two inches on either side at right angles to the fracture of the blade-stub.

A section was also taken parallel to the fracture and 1/2 in. beneath the fracture and was examined to determine if the fracture was in any way related to weld repairs. Several welds and one welded-up "hot-tear" were observed but these did not appear to relate to the fracture. (Examination of the hot-tear and one associated shrinkage cavity is discussed later.)

Deep Etch and Sulphur Prints - Examination of Welds Relative to the Fracture Surface

Figure 7 illustrates a sulphur print taken on the ground section 1/2 in. beneath the fracture (i.e., the fracture is directly beneath the section illustrated.)

TABLE 1

Chemical Analysis

Sample	Element (Per Cent)											
	C	Mn	Si	S	P	Ni	V	Acid Sol Al	Cu	Sn	Cr	Mo
1963 Specification*	.20 max	.75/1.10	.50 max	.020 max	.025 max	1.5 min	.12 max	0.020 max	-	-	.20 max	-
Blade	.21	.83	.45	.023	.004	1.76	.09	<.005	.15	.014	.14	.05
Tip	.18	.86	.41	.023	.005	1.74	.08	.002**	.18	-	.09	.02

*Specification revised June 1966.

**Total aluminum <0.005%.

The welds are marked by arrows (No. 1); these are visible because of the extra low sulphur content of the weld deposit. No cracks or defects were observed at the welds. These welds had been made prior to heat treatment and were only detected by sulphur printing since the weld microstructure closely matched that of the casting and, unlike the superficial hub welds, the weld deposits had not become etched or differentially attacked during salt water service.

Figure 7 illustrates part of a self-welded, hot-tear (arrow No. 2) which connected with a 3/8 in. diameter shrinkage cavity 2 in. beneath the casting surface. This was the only shrinkage cavity observed in any of the sections and in this instance appeared to result from last-freezing, segregated metal, filling a hot-tear (self-welding).

Figure 8 illustrates sulphur prints and deep-etches on a section normal to the fracture surface. (Note that sulphur print and deep-etch photograph prints are reversed during processing.)

Figure 9 shows a section in the hub region matching the section illustrated in Figure 8. The casting appears sound and normal with respect to distribution of sulphides, macrostructure and absence of shrinkage.

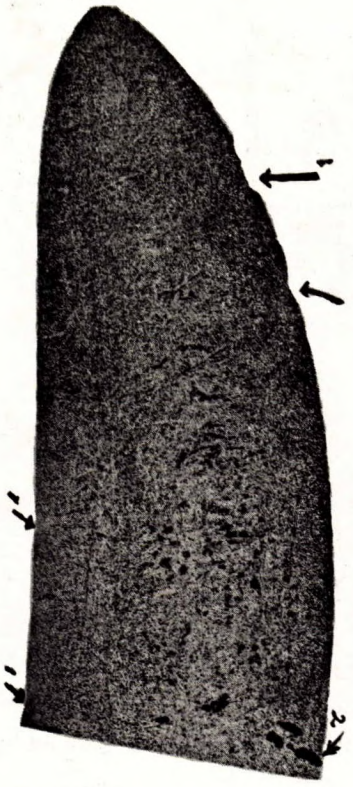

X 1/7 approx.

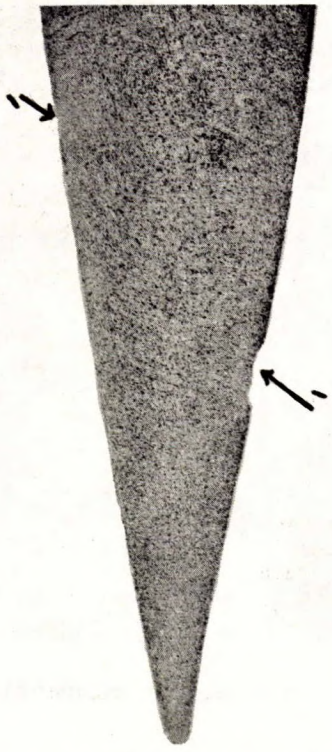

Figure 7. Sulphur Print of Section Directly Beneath Fracture Surface. Welds are shown (arrows, No. 1). Part of a "healed" hot-tear, having a diameter of approximately 1/2 in. and a length of 2 in. is illustrated, (arrow No. 2). Figures 16 to 19, inclusive, also illustrate this hot-tear in the polished and etched condition. Chemical analysis showed phosphorus segregation in this area.

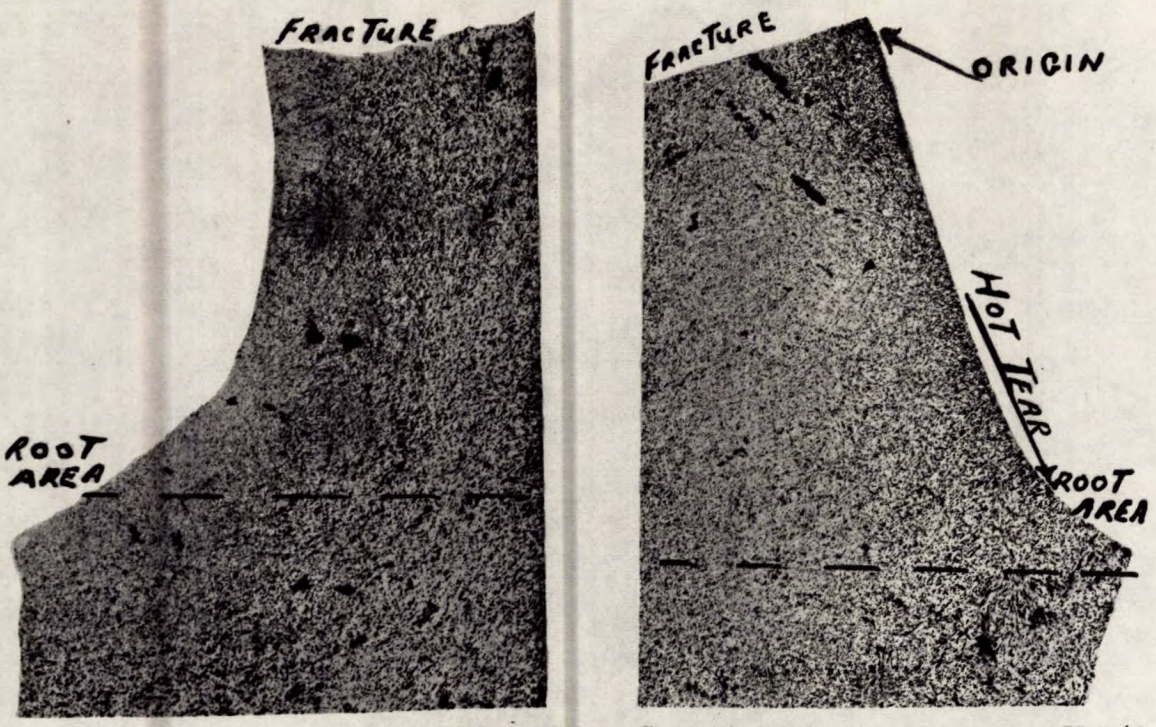

(a) S print - Shows S segregation. X 1/3

(b) Deep-etch - Shows macrostructure. X 1/3

Figure 8. Section Normal to Fracture at Origin. Sulphur print (a); same section deep-etched, HCl: water, (b). The fracture surface and origin side is marked. Also illustrated is a typical welded hot-tear in the root area which nevertheless did not contribute to the fracture.

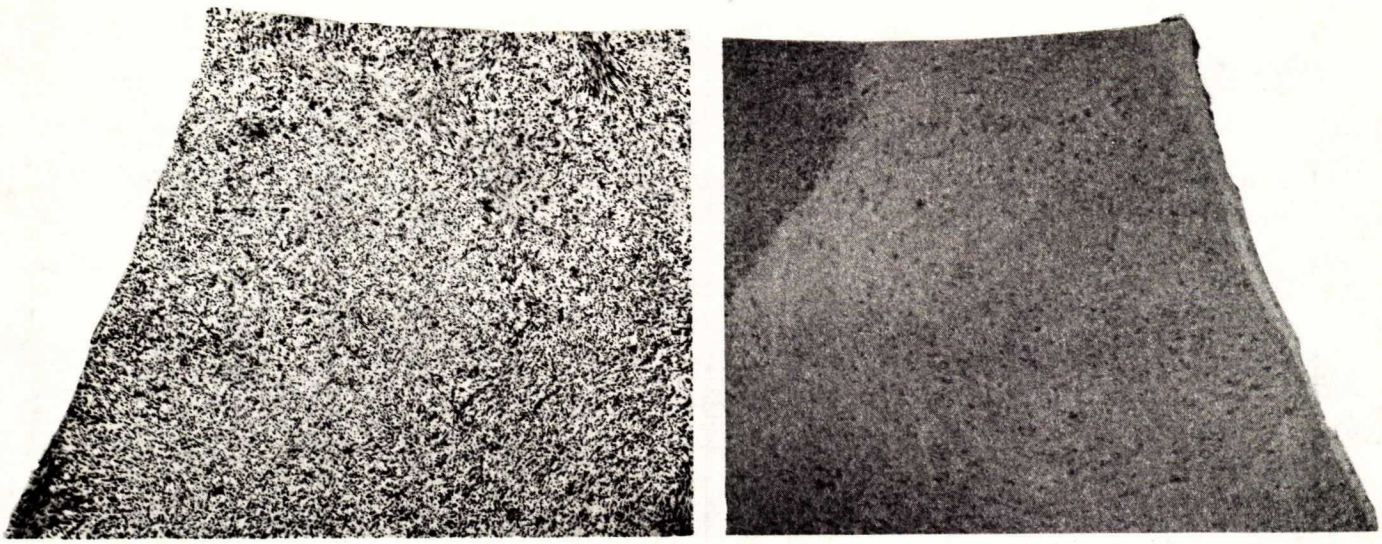

Sulphur Print, Hub Region. (a) Deep-Etch, Hub Region.

Section is below and matches the right half-section shown in Figure 8.

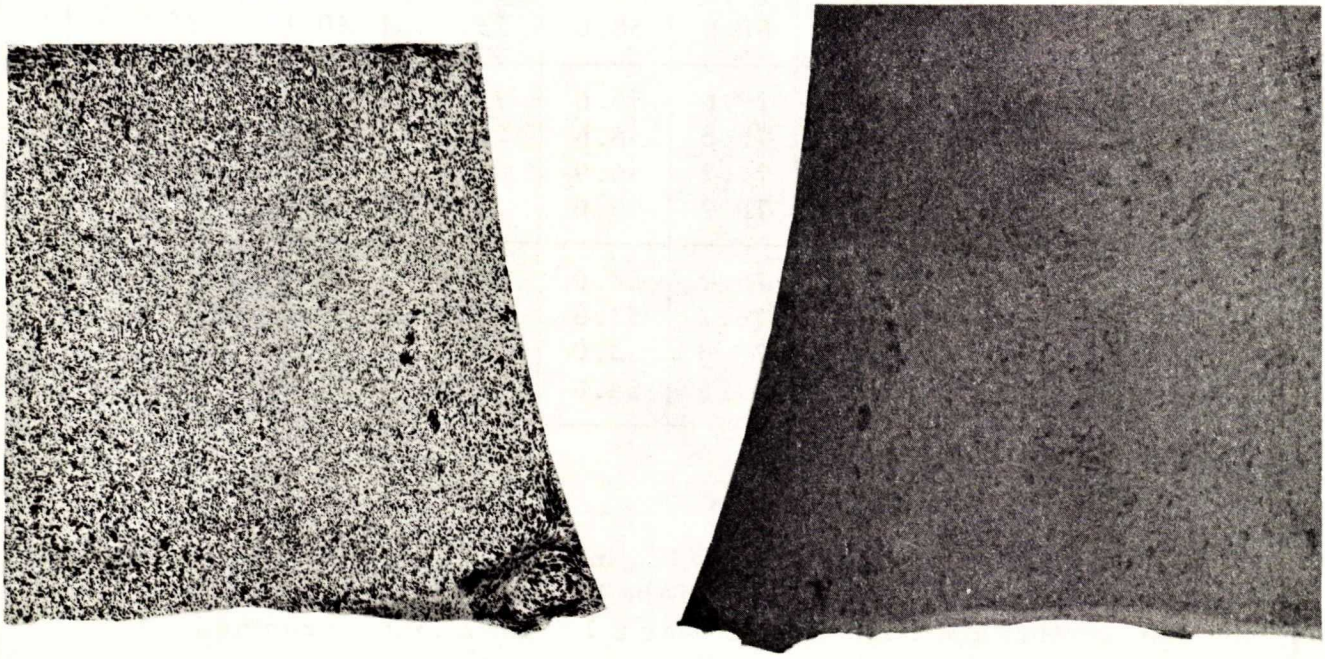

Sulphur Print, Hub Region. (b) Deep-Etch, Hub Region.

Figure 9. Sections Illustrating Sulphide Inclusion Content and Macrostructure of Hub Region. Adjacent to sections shown in Figure 8 (i.e., this section is normal to the fracture surface).

Mechanical Tests

The results of tensile tests made on metal from the surface and centre of the blade, stub and from the centre of the hub section are listed in Table 2.

TABLE 2

Tensile Tests
(0.505 in. diameter test bars)

Location of Test Bars (A-L inclusive)	Bar	UTS kpsi	Yield kpsi	% El in 2 in.	RA %	BHN 3,000 kg load
Blade - Working Section - 1-1/2 in. from surface.	A	80.8	56.4	29.5	48.9	170
	B	80.6	57.0	29.5	51.9	175
	G	79.6	58.6	19.5	32.8	180
	H	80.0	58.0	26.0	40.1	170
Blade - Working Section - centre of section.	C	79.6	55.0	17.5	7.3*	180
	D	79.6	58.6	26.0	36.0	170
	E	77.7	55.9	16.5	31.1	170
	F	78.9	55.0	21.5	32.5	170
Hub - Centre of Thick Section	I	75.7	52.0	18.5	28.8	166
	J	76.7	53.6	15.5	29.2	162
	K	76.5	53.0	20.5	28.5	170
	L	74.3	54.0	14.0	21.3	166

* defect in tensile bar.

Two bend samples 8 in. x 1/2 in. x 1-1/2 in. (167 BHN) were cut at the root region with the centre of the bend corresponding to the centre of the root section and were U-bent over a 1/2 in. diameter radius.

Both bars were bent through 135 degrees over a 1/2 in. diameter form without rupture. The crack, open approximately 1/4 in. on the tension side, showed a tough, fibrous fracture (at room temperature) except for one 1/8 in. diameter "fisheye" on each fracture. Similar "fisheyes" were observed on all tensile bars except those from the 1-1/2 in., "surface", position.

Drop-Weight and Charpy V-Notch Results

The Charpy V-notch, impact-temperature curve was obtained for temperatures between +80°F and -80°F. The results are shown in Table 3.

TABLE 3

Charpy V-Notch Impact Results
(ft-lb)

Temp °F	-80°F	-60°F	-40°F	-20°F	+20°F	+80°F
Bar 1	12	12	40	40	46	66
" 2	16	16	28	26	50	72
" 3	6	26	29	28	44	75
% Cleavage Fracture (visual estimate)						
Average ft-lb	11.	18.	32.	31.	47.	71.
% Cleavage*	100%	97%	95%	90%	60%	30%

*Estimated % fine cleavage according to ASTM A443-64.

Twenty-four bars, 3/4 in. x 2 in. x 5 in., containing the standard notched weld bead were broken by drop-weight testing. The NDT temperature was -15°F, which was below the service temperature but was considerably higher than the -70°F NDT temperature obtained with minimum carbon silicon or vanadium in laboratory tests shown in Appendix 1. No difference was observed between the NDT temperature measured on bars from the blade-stub B-1 to B-6 inclusive, from the root area of the broken stub-samples R_7 to R_{14} inclusive, and from the thick hub region samples H-15 to H-24 inclusive. NDT determined according to ASTM E-208 using 3/4 in. x 2 in. x 5 in. bars, 200 lb weight, 360 ft-lb energy, except that deflection was 2.5 mm instead of 1.5 mm.

Metallographic Examination

The microstructure of the hub of the broken blade is illustrated in Figure 10.

Figure 11 illustrates the microstructure observed at the trailing edge of the blade-stub taken at the fracture surface.

Figure 12 illustrates the microstructure at the thick section taken at the apparent origin as indicated by the chevron markings, visible on the fracture surface.

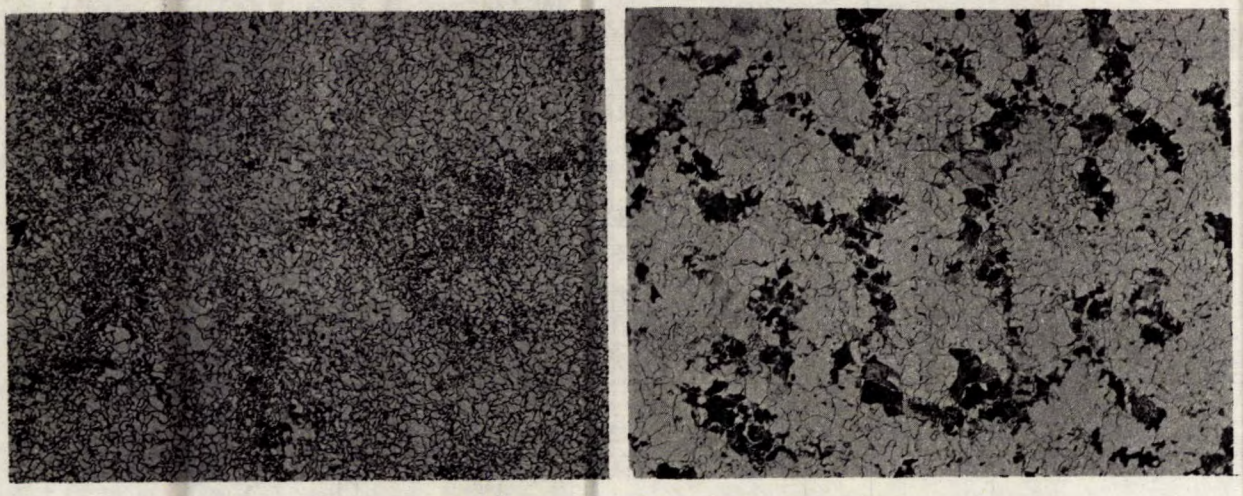

(a) X100 - 2% Nital Etch (b)

Figure 10. Surface (decarburized) (a); and General Microstructure (b), respectively of "Blade-Tip" Sample. Note that the general microstructure illustrated in Figure 10(b) resembles that of the "blade-stub" shown in Figure 11.

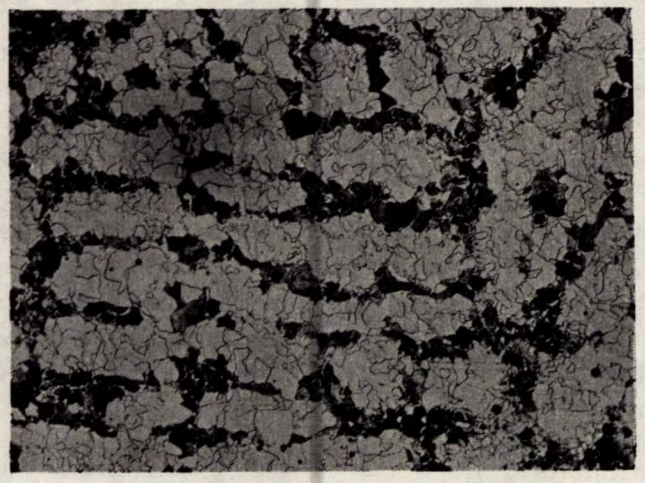

X100 - 2% Nital Etch

Figure 11. Dendritic Ferrite-Pearlite Microstructure at the Thin Section, Trailing Edge, Intersecting the Fracture of the "Blade-Stub" Sample. The general microstructure of this casting resembles that of the "blade-tip" sample.

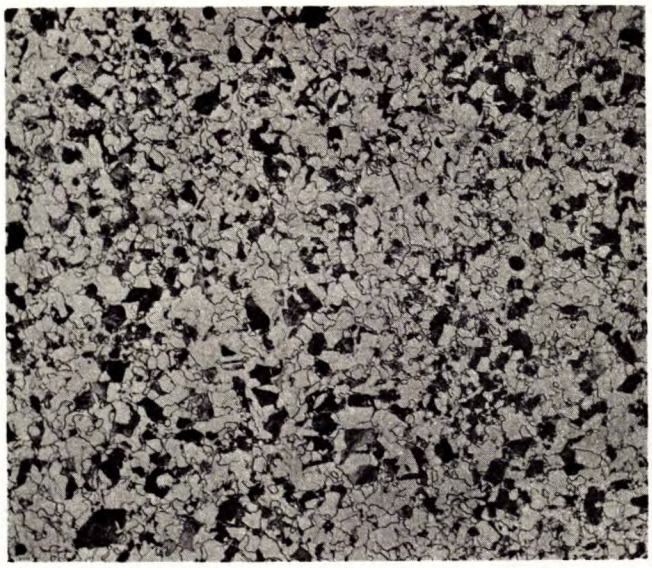

X100 - 2% Nital Etch

Figure 12. Ferrite-Pearlite Microstructure at the Fracture Origin, "Blade-Stub".

Figure 13 illustrates a grain boundary and sulphur segregation observed in the root area of the broken blade-stub.

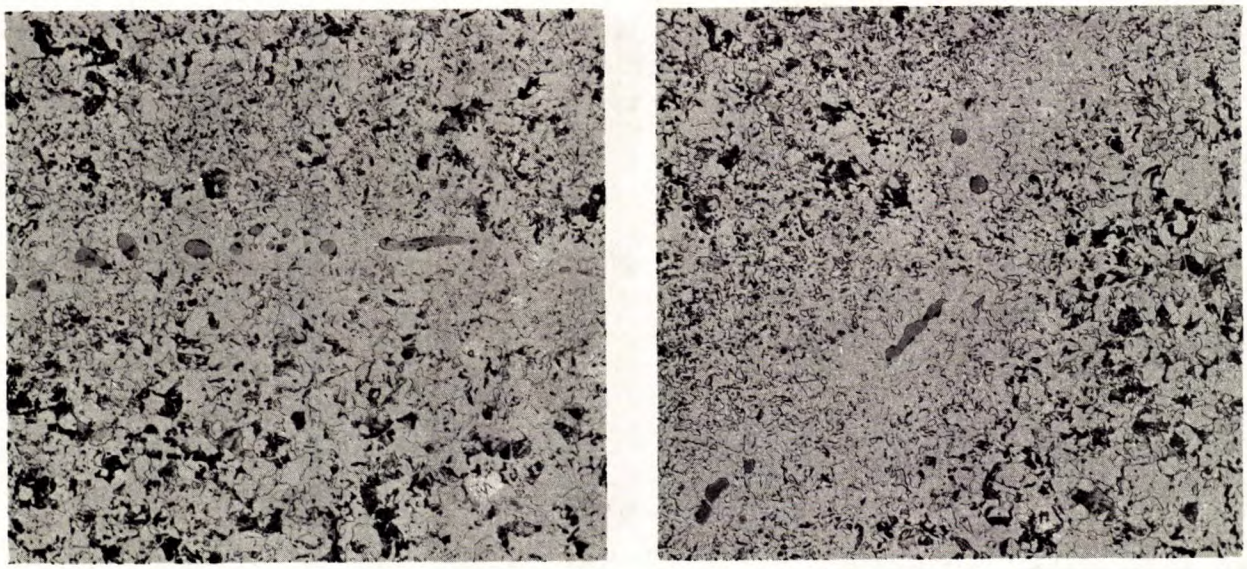

(a) X100 - 2% Nital Etch (b)

Figure 13. Microstructure and Sulphide Distribution at "Blade-Stub" Grain Boundary in the Root Area are Illustrated.

Figure 14 illustrates typical silicate (deoxidation) inclusions observed in the blade-stub casting. Figures 15(a) and (b) illustrate duplexed silicate inclusions and one MnS inclusion viewed in the as-polished condition under white light, Figure 15(a), and under polarized light, Figure 15(b).

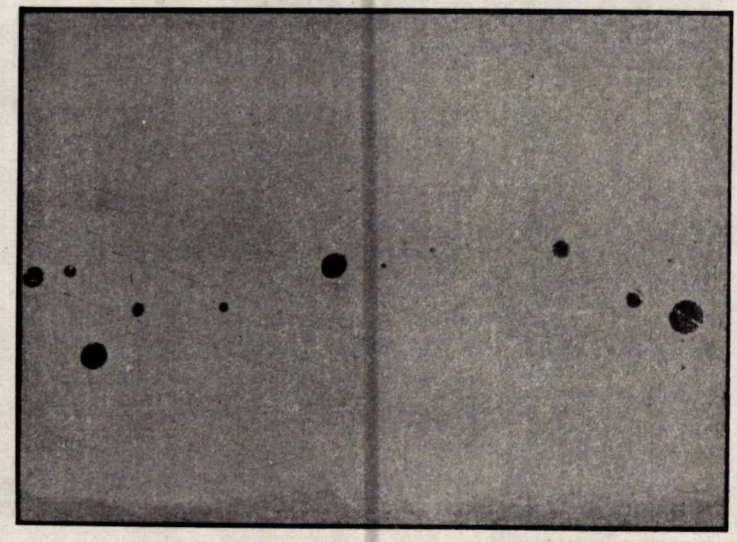

X100 as-polished

Figure 14. Silicate (Deoxidation) Inclusions, Observed in "Blade-Stub" Casting.

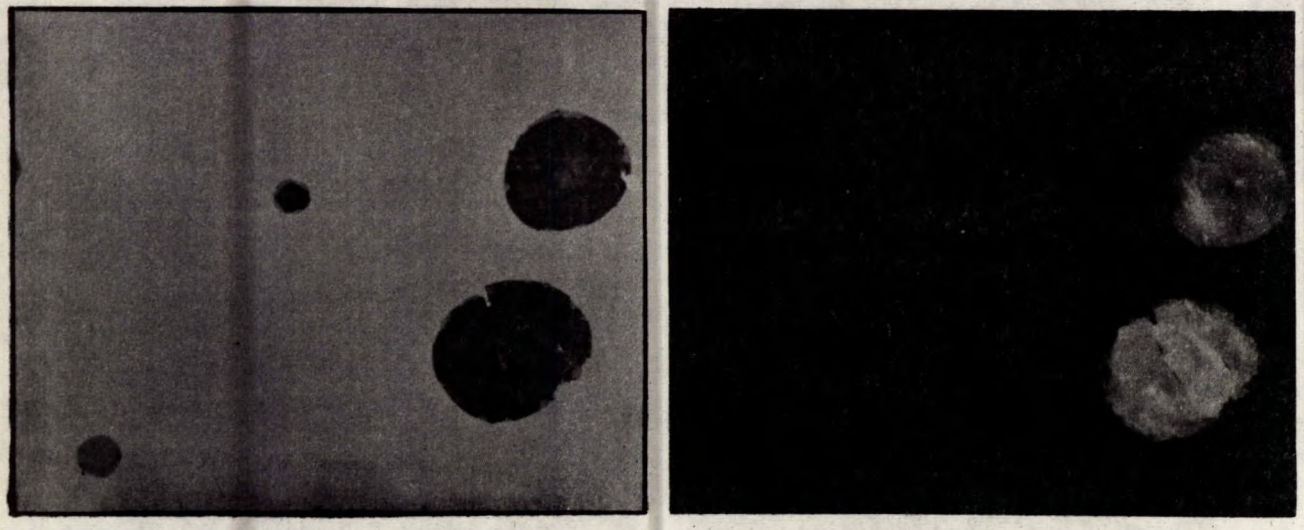

(a) as-polished, white light (b) as-polished, polarized light

Figure 15. Illustrates Typical Spherical Silicate-type and One MnS type Inclusions, Observed in Propeller "Blade-Stub" Casting. The silicate inclusions are frequently duplexed with MnS at their outer surface.

"Self-Healed" Hot-Tear Observed on Section 1/2 in. Below and 2 in. from Apparent Origin of Fracture.

The appearance of the hot-tear on a polished section 1/2 in. beneath the fracture, 1/2 in. from the surface, and 2 in. from the apparent fracture origin, is illustrated in Figure 16 at low magnification.

X4

Figure 16. Healed Hot-Tear Extending Inwards at 45 Degrees from Cast Surface, 2 in. from the Fracture Origin. Last-freezing metal from 2 in. inside the casting flowed into the tear filling it and leaving a 3/8 in. diameter shrinkage hole at the 2 in. position. Apparently the tear formed and healed itself after a 2 in. thick skin (skull) had formed on the surface of the casting and after effective feeding of metal from the riser had ceased.

The area illustrated in Figure 16 was enriched with respect to phosphorus, from 0.004% to 0.116% as shown by wet chemical analysis of drillings from the segregate. Microprobe analysis showed that the grain boundaries were filled with MnO. Microshrinkage and areas of phosphide eutectic were also observed and were consistent with the defect having been healed by inflow of segregated, last-freezing, metal. The defect was not a weld and there was no possibility of, or evidence of weld preparation; also, weld deposits were all typically low with respect to sulphur, whereas sulphur and phosphorus segregation was observed in this area both by wet analysis and by sulphur printing, as illustrated in Figure 7.

Analysis of drillings from the segregate areas, illustrated in Figure 16, gave the results shown in Table 4.

TABLE 4

Results of Wet Analysis of Drillings from Hot-Tear Segregate

Area	Mn	Si	S	P
Segregate Area (Figure 16)	0.77	0.75	0.043	0.116
Matrix Analysis (Table 1)	0.83	0.45	0.023	0.004

Metallographic and microprobe examination showed that in this area phosphorus was segregated sufficiently to form steadite, and manganese to form MnO films in grain boundaries. Sulphur and silicon were also segregated.

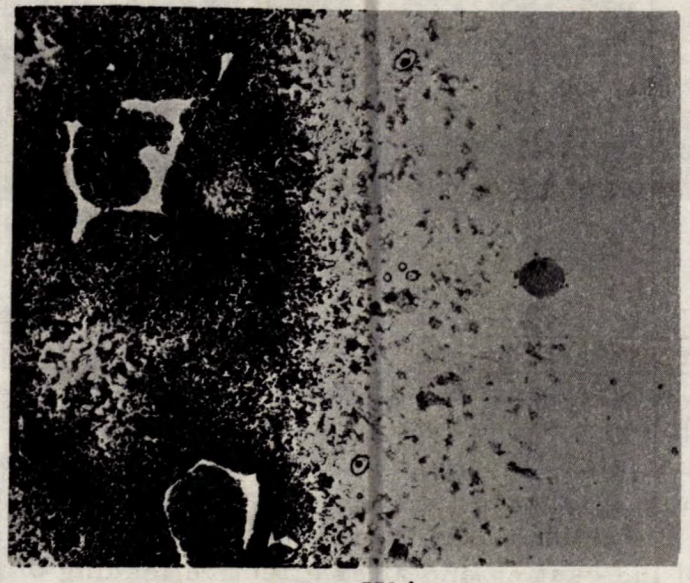

X36

Picric Acid + Sodium Tridecyl Benzene Sulphonate Etch

Figure 17. Illustrates Interface Between Matrix and Segregate. Part of segregate area shown at the left of Figure 16.

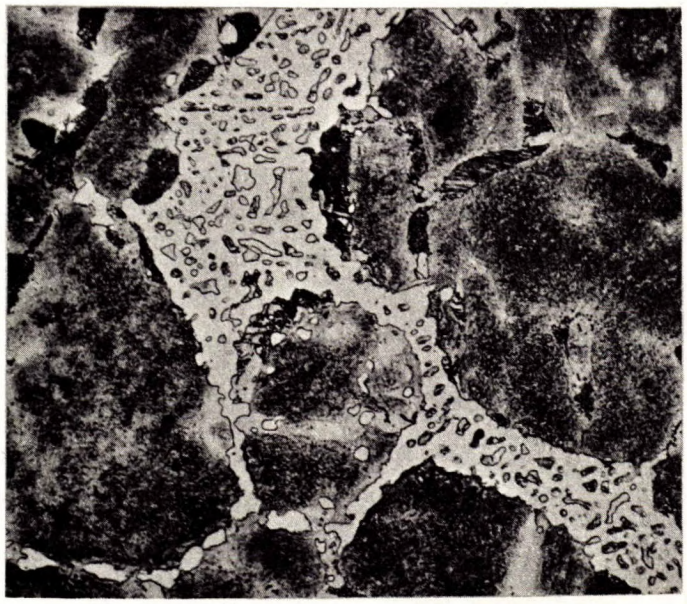

X500

Picric Acid + Sodium Tridecyl Benzene Sulphonate Etch

Figure 18. Illustrates Phosphorus Segregation in Hot-Tear Region. Phosphorus segregation has occurred to the extent that phosphide eutectic "Steadite" is visible in the microstructure.

Figure 19 illustrates manganese segregation in the grain boundaries and inclusions in the hot-tear segregate area.

(a) X100, as-polished

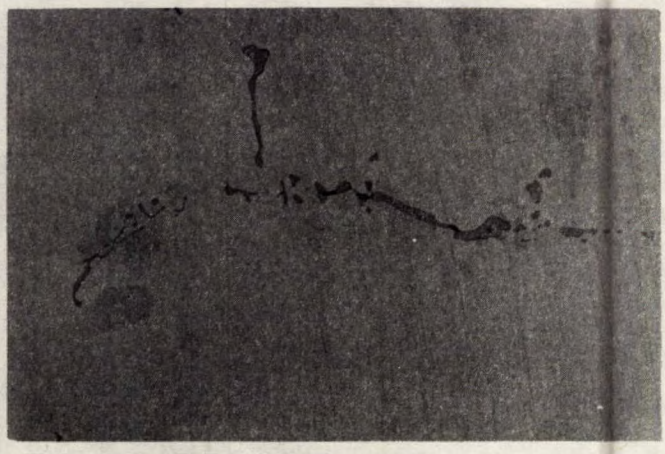

(b) X100, as-polished

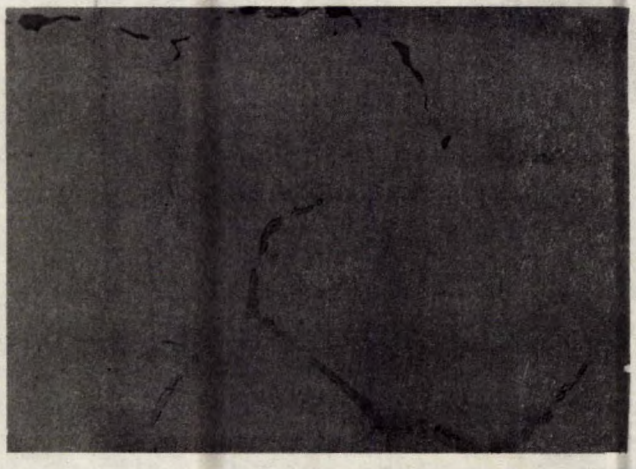

(c) X100, as-polished

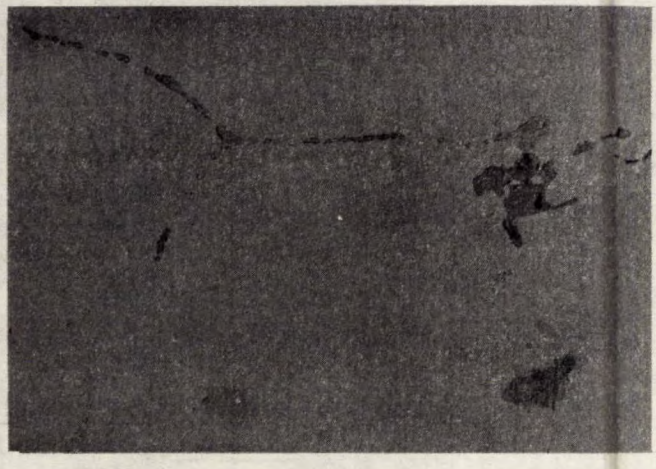

(d) X100, as-polished

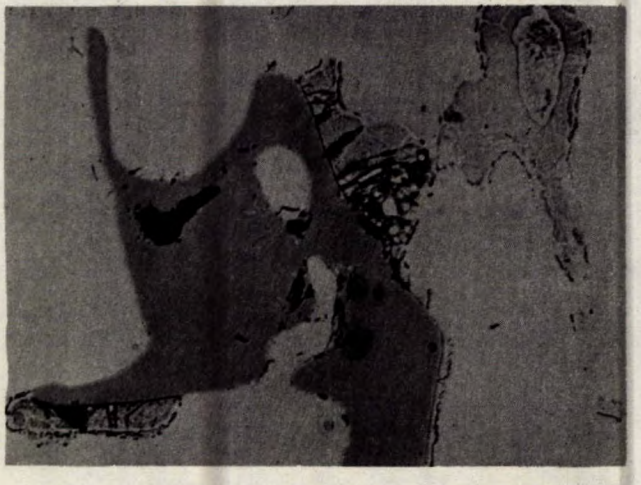

(e) X500, as-polished

(f) X500, as-polished

Figure 19. Mn Segregation at Grain Boundaries (a) to (d) Inclusive. Inclusions in segregate area are illustrated (c) and (f). Microshrinkage was also observed.

DISCUSSION

Examination of the fracture indicates that both the "blade-stub" and "blade-tip" fractures were due to impact. The "blade-stub" fracture had chevron markings, a well-defined origin and showed little deformation; the part of the "tip" fracture observed showed a shear lip indicative of considerable ductility at fracture.

The steel compositions were both close to specification except that the carbon was at the maximum level in the blade sample. The drop-weight tests showed that the NDT temperature of the blade sample was only -15°F, whereas under test conditions and with vanadium-free steel optimum NDT temperatures of -75°F were obtained (in 6 in. x 7 in. x 13 in. test blocks).

Figures 20 and 21 illustrate the effect of vanadium, nickel and silicon on NDT as observed in laboratory tests on 6 in. x 7 in. x 13 in. block castings. These results indicated no advantage for use of vanadium in heavy cast sections particularly when the austenitizing temperature was restricted to 1600-1700°F by hazard of excessive blade distortion.

The castings were sound and gave mechanical and Charpy V-notch results in excess of specification requirements. Despite the relatively high Charpy V-notch energy values obtained on the failed casting, the Charpy bar fractures showed cleavage areas both at room temperature and at sea water temperature +20°F.

Metallographic examination showed a dendritic distribution of pearlite in the cast section except in areas where weld repairs had preceded heat treatment.

The fracture did not appear to be related to the presence of any weld defect -- in fact, all welds observed were only traceable by their lower sulphur content in comparison to matrix metal.

A welded hot-tear defect was observed about 2 in. from the apparent origin of the fracture, but did not appear to have been directly related to the fracture. (This defect was unusual and for this reason considerable attention was paid to it -- it appeared to be a self-healed hot-tear containing microshrinkage, phosphorus segregation as steadite, manganese segregation as oxide, and sulphur segregation.)

CONCLUSIONS

(1) Both of the failed castings met the requirements of the specification with respect to chemical composition.

(2) The "blade-stub" casting met the requirements of the specification with respect to tensile properties, Charpy V-notch energy value, and the tests pertaining to good workmanship - feeding, surface finish, and weld repairs, with the possible exception of one segregate area. (This area did not appear to have contributed to failure.)

(3) Failure appeared to have resulted by brittle fracture at sea water temperature under application of a large impact force. Chevron markings were observed on the fracture surface and the stub fracture showed little deformation. The tip fracture showed a 1/8 in. shear lip, suggesting that more deformation occurred in this casting. (Determination of NDT temperature was not possible for this sample because of the small quantity of metal available.)

(4) The drop-weight, NDT temperature determined for the failed casting was only -15°F, whereas under some conditions of heat treatment, or, without vanadium, 2% nickel cast steel blocks (6 in. x 7 in. x 13 in.) gave NDT temperatures of the order of -75°F.

RECOMMENDATION

(1) The NDT temperature of the cast metal should be as low as possible to obtain maximum ductility at sea water temperature under impact load conditions. The specification has been revised to eliminate the vanadium addition since proper heat treatment of vanadium steel is difficult on account of blade distortion. Minimum silicon content and low carbon should provide -45 to -75°F NDT temperature for 2% nickel cast steel.

APPENDIX 1

The results of an experiment made on 6 in. x 7 in. x 13 in. block castings, heat treated by normalizing from 1700°F and 1550°F, followed by 1100°F tempering treatment were reported in Internal Report PM-R-66-9.

A summary of the compositions tested and drop-weight NDT temperature obtained in comparison of the effect of vanadium at 0.10% and 0.20%; of silicon at 0.10% and 0.50%; and of nickel at 1.8% and 3.0% are summarized in Figures 20 and 21. The NDT temperature was increased with increase of hardness due to secondary hardening by vanadium after tempering and by solution-hardening of nickel at the 3% level.

Lowest NDT temperatures were obtained in melts containing no vanadium and in those in which carbon, silicon and vanadium were at minimum levels. Increase of silicon also appeared to increase NDT temperature, particularly when the silicon content was in excess of 0.30%. The silicon effect on low temperature toughness was further increased in the range 0.50% to 0.80% silicon.

Figures 22 and 23 illustrate the dendritic (cored) appearance of a laboratory high silicon, high carbon, high vanadium melt (72) having an NDT temperature of 18°F and a ferrite pearlite microstructure obtained in 2% nickel steel which had a NDT temperature of -75°F No. 2512.

Three vanadium-free melts in addition to 2512 were cast as 6 in. x 7 in. x 13 in. blocks for check determination of NDT. Castings from these melts (2750, 2752, 2755) were tested after furnace annealing from 1550°F and tempering at 1100°F. Melt 2512 was tested in the double normalized (1725°F, 1550°F) tempered 1100°F condition. NDT results, heat treatments and chemical compositions are listed in Tables 1A and 2A respectively.

TABLE 1A

NDT - (200 lb Hammer - 360 ft-lb Energy - 2.5 mm Deflection)

Melt No.	.02% sol Al	.06/.10% sol Al
2512 (DNT)	-72°F	-75°F
2750 (AT)	-31°F	-50°F
2752 (AT)	-31°F	-40°F
2755 (AT)	-40°F	-40°F

(DNT) - 1725°F 15 min, air cool, 1550°F 15 min air cool. Temper 1100°F, 2 hr, air cool.

(AT) - heat to 1550°F held 2 hrs at 1550°F, furnace cooled, tempered 4 hr at 1100°F.

TABLE 2A

Chemical Composition and Heat Treatment of 2% Nickel Steel Castings

Melt	Heat Treatment	Hardness BHN	C	Mn	Si	S	P	Ni	V	sol Al
2512-1	(DNT)	165	.18	.85	.24	.014	.012	1.94	Nil	<0.02
2512-2	"	170	"	"	"	"	"	"	"	0.10
2750-1	(AT)	165	"	.69	.12	.020	.011	1.8	"	0.02
2750-2	"	"	"	"	"	"	"	"	"	0.06
2752-1	"	"	.22	.84	.31	.012	.016	"	"	0.02
2752-2	"	"	"	"	"	"	"	"	"	0.06
2755-1	"	"	.17	.88	.32	.015	.030	"	"	0.02
2755-2	"	"	"	"	"	"	"	"	"	0.06

DEP:DAM:bb

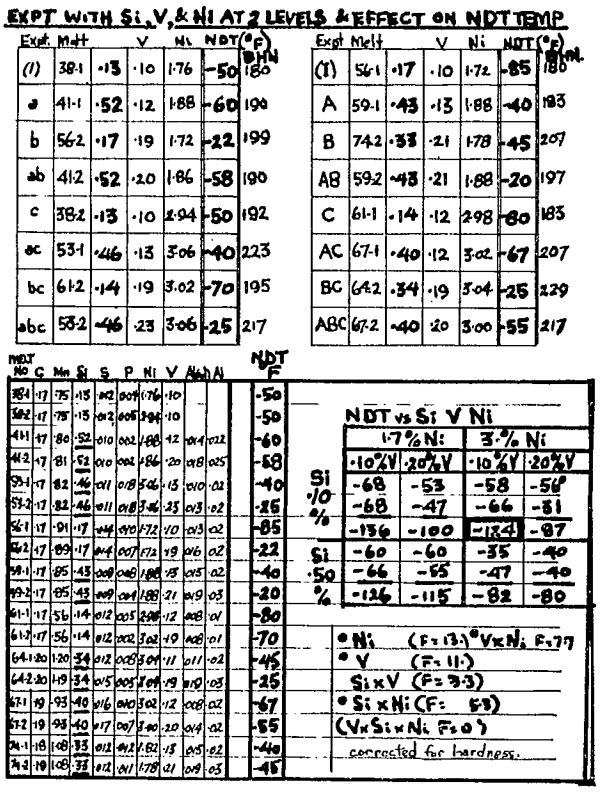

Figure 20. Laboratory Melts, 2 Levels V, Ni, Si and NDT Temperatures Obtained by Drop-Weight Tests.

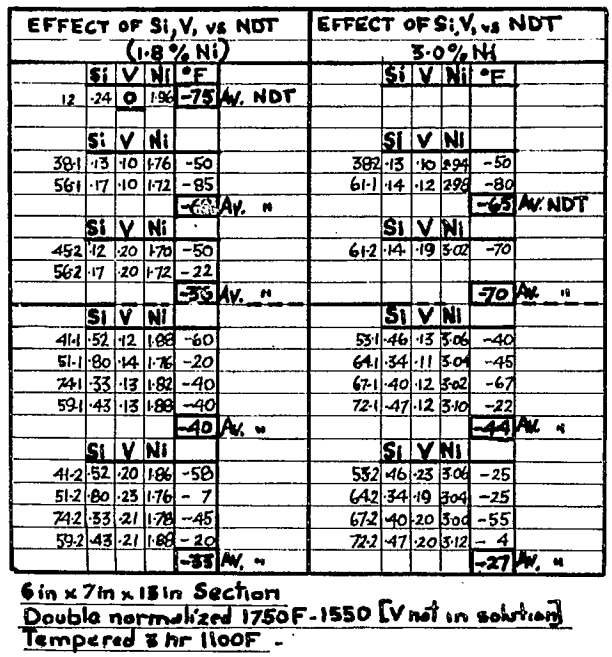

Figure 21. Data from Figure 20, Summarized. Note that 2% nickel cast steel at minimum V and Si content has minimum NDT temperature -75°F.

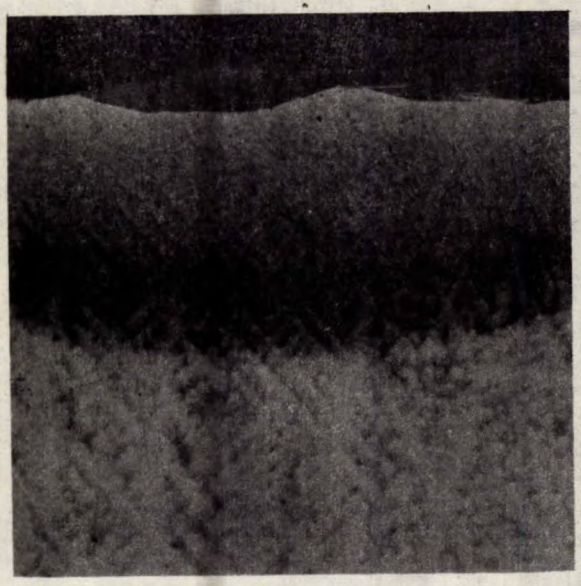

(a) X10

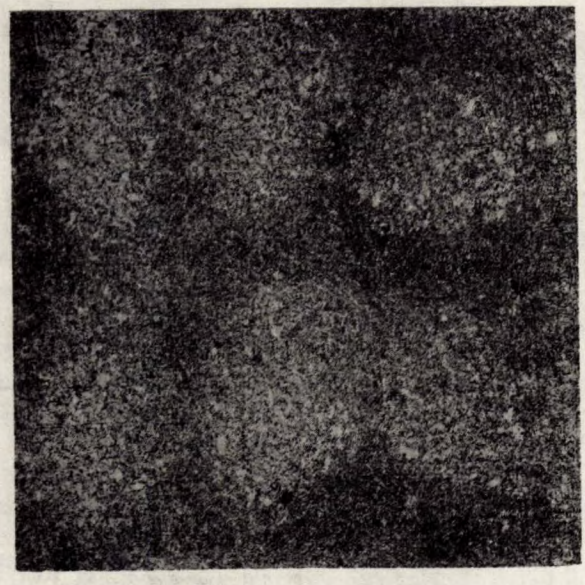

(b) X100

Figure 22. NDT Temperature -5°C (+18°F), Melt 72-2. Vanadium, carbon, silicon at high side of specification. Figure 22(b) illustrates the fine-grained cored microstructure which gave cleavage-type fracture on Charpy V-notch test bars at ambient temperature.

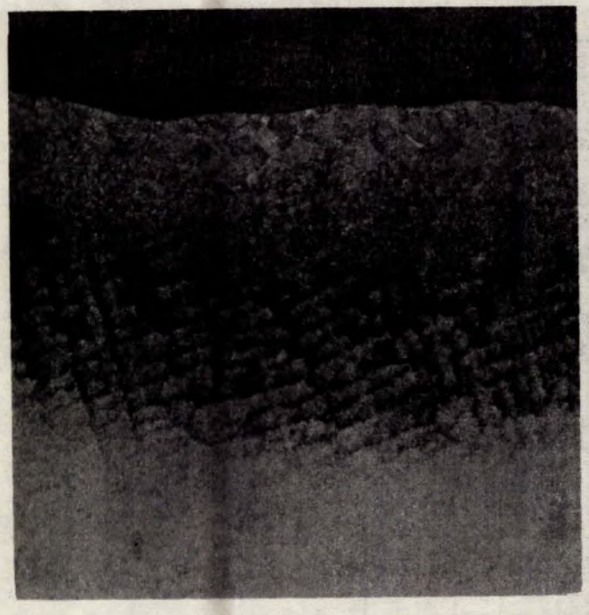

(a) X10

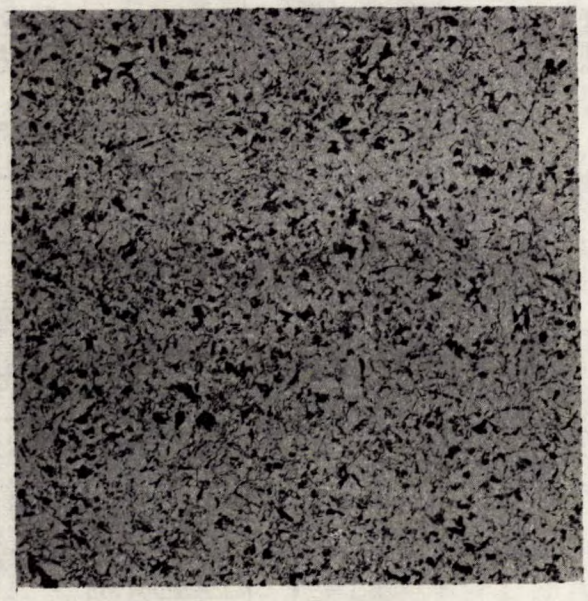

(b) X100

Figure 23. NDT Temperature -65°C (-75°F), Melt No. 12. No vanadium, carbon and silicon at low level. Figure 23(b) illustrates homogeneous, pearlite-ferrite microstructure which gave fibrous fracture in Charpy V-notch test bars at ambient temperature.